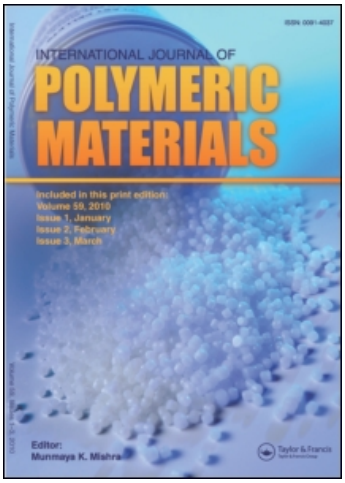

International Journal of Polymeric Materials
Publication details, including instructions for authors and subscription information:
http://www.informaworld.com/smpp/title~content=t713647664

Thermal, Mechanical and Rheological Properties of Polypropylene/Poly(ethylene-co-methyl acrylate) Blends

Ahmed E. Bishara[a]; Habib I. Shaban[a]
[a] Chemical Engineering Department, Kuwait University, Safat, Kuwait

Online publication date: 04 December 2009

To cite this Article Bishara, Ahmed E. and Shaban, Habib I.(2010) 'Thermal, Mechanical and Rheological Properties of Polypropylene/Poly(ethylene-co-methyl acrylate) Blends', International Journal of Polymeric Materials, 59: 2, 134 — 149
To link to this Article: DOI: 10.1080/00914030903231159
URL: http://dx.doi.org/10.1080/00914030903231159

International Journal of Polymeric Materials, 59:134–149, 2010

ISSN: 0091-4037 print/1563-535X online
DOI: 10.1080/00914030903231159

Taylor & Francis
Taylor & Francis Group

Thermal, Mechanical and Rheological Properties of Polypropylene/ Poly(ethylene-co-methyl acrylate) Blends

Ahmed E. Bishara and Habib I. Shaban

Chemical Engineering Department, Kuwait University, Safat, Kuwait

Isotactic polypropylene (PP) has been blended with poly(ethylene-co-methyl acrylate) (EMA) (75/25 wt/wt%) in a single-screw extruder. The compatibilizing effect of polypropylene grafted with maleic anhydride (PP-g-MAH) has been examined. The nonisothermal crystallization of the developed blends has been investigated using differential scanning calorimetry (DSC) and analyzed using Avrami, Tobin and Liu models. The thermal stability of the blends was assessed through thermogravimetric analysis (TGA). The tensile and impact properties, as well as the melt viscosity, have also been determined. The presence of rubber accelerates the crystallization of PP. The thermal stabilities of the blends are intermediate between those of their constituents. Tensile strength and modulus are reduced upon incorporation of EMA into PP, but ultimate elongation and impact strength are improved. The melt viscosity variation with shear rate for all the systems was typical of shear-thinning behavior. The compatibilizing agent has a pronounced effect on enhancing the thermal and mechanical properties of the blend.

Keywords poly(ethylene-co-methyl acrylate), polymer blends and alloys, polymer characterization, polypropylene

---

Received 13 July 2009; in final form 20 July 2009.
The authors would like to thank the Research Department at Kuwait University for funding this research through project EC 04/07. The authors are also grateful to Dr. Mathew Johnson, Senait Asmerom and Joyson John for the scientific assistance they have provided.
Address correspondence to Prof. Habib I. Shaban, Chemical Engineering Department, Kuwait University, P.O. Box 5969, 13060 Safat, Kuwait. E-mail: habibshaban@gmail.com

INTRODUCTION

Polypropylene (PP) is a semi-crystalline, thermoplastic polyolefin that offers a very attractive combination of physical and mechanical properties at a relatively low cost. This makes it a versatile material with a continuously increasing number of applications. However, in some cases, not all the characteristics of this material are suitable for common service conditions. For instance, PP exhibits poor low-temperature impact resistance because of its high transition temperature and high crystallinity [1–4].

Elastic modulus and impact strength are two critical properties in many engineering design applications. Most structural designs rely heavily on material stiffness to provide the desired properties to the structure. Impact strength is critical in resisting repeated impacts encountered in sectors like transportation and consumer products. Unfortunately, high stiffness and high toughness are often properties not found in the same material. Polystyrene and poly(methyl methacrylate) are two examples of high modulus materials that have limited impact resistance, whereas polyethylene and polypropylene are tough materials (i.e., exhibit high ultimate elongation) that have poor stiffness. Exceptions exist, of course, such as polycarbonate, which possesses good stiffness and toughness. Blending and copolymerization are viable approaches to formulating polymeric materials with enhanced stiffness and toughness [5].

Polypropylene (PP)/thermoplastic elastomer blends have been investigated thoroughly to achieve properties tailored to particular applications [6–10]. The blending of a thermoplastic and an elastomer gives a class of rubbery materials known as thermoplastic elastomers. These materials possess the good physical properties of elastomers and the excellent processing characteristics of thermoplastics. Among the various types of thermoplastic elastomers, those prepared by melt-mixing of a crystalline thermoplastic material and an elastomer under high shearing action have gained considerable attention due to the simple method of preparation and relatively easy attainment of the desired physical properties by varying blend ratios [11–13].

Studies of PP-elastomer copolymer systems often involve ethylene-propylene rubber (EPR) [14,15], ethylene-propylene-diene terpolymer (EPDM) [16], and styrene-ethylene- butylene-styrene block copolymers (SEBS) [17,18]. Poly(ethylene-co-vinyl acetate) (EVA) and poly(ethylene-co-methyl acrylate) (EMA) also provide alternatives to conventional impact modifiers. Blends of PP and EVA, made by the crosslinking of the elastomeric phase with dicumyl peroxide, were investigated by Thomas [19] and Valera-Zaragoza et al. [20]. These polymers were completely miscible with each other and crosslinking was carried out *in situ* via transesterification reaction during the extrusion process. The crosslinking during mixing improved the mechanical properties; however, some degradation of PP blends with a crosslinked or noncrosslinked EVA and EMA phase were reported by other researchers [21,22].

The polar EMA is immiscible with the nonpolar PP and blending them may change the crystal structure of PP through changing the heterogeneous nucleation activity. Nonetheless, toughening with polar elastomers can provide better adhesion properties at the surface. This is done by controlling the dispersed elastomer particle through adjusting interfacial energy, polymer properties and volume fractions of the blend components. The generation of non-bonded phase boundaries has both positive and negative ramifications for blend properties. Such interfaces are excellent crack deflection sites that can stop or deflect fast propagating cracks in brittle polymers such as polystyrene. On the other hand, non-bonded interfaces prevent load transfer across the interface, thus weakening the material. The preferred remedy for such blends is to use compatibilizers to bond the phases. In such compatibilized blends the phase bonding substantially improves the impact toughness, but in many cases the modulus and time-dependent properties (e.g., creep) are sacrificed. Yet, in some prominent cases the impact strength of the material is enhanced without loosing tensile and flexural strength. Several polar monomers, such as oxazoline, mercapto, cyanate ester and maleic anhydride have been investigated. Among them, the most studied modifications of polyolefins are those with maleic anhydride and alkyl maleates, which are performed in solution, solid state or melt state [5].

Avrami [23] is the most widely used model in studying polymer crystallization. But in many cases, the experimental situation is complicated by different phenomena taking place during the course of crystallization. Thus, the interpretation of the experimental data with the Avrami model leads to either large or fractional values of the Avrami exponent and deviations from the experimental data at the final stages. This could be due to the simple assumptions made by Avrami model, such as constant radial growth, absence of secondary crystallization, exclusivity of nucleation, and constant shape of the growing crystal. Many researchers, such as Malkin et al. [24] and Tobin [25], have attempted to develop models to modify the Avrami equation, taking into account the complex nature of polymer crystallization (i.e., a combination of primary and secondary crystallization processes). According to Ozawa's theory [26], the nonisothermal crystallization process is a result of infinitesimally small isothermal crystallization steps. Liu et al. [27] have also developed a method by combining the Ozawa and Avrami equations.

Avrami and Tobin models have been applied to study the isothermal crystallization of nylon 6/PEGMA blends [28], poly (ethylene terephthalate) (PET) [29], and polypropylene [30]. Avrami model has also been utilized to characterize the nonisothermal crystallization of polymeric systems such as polyethylene [31], poly(butylene terephthalate) (PBT) [32] and polyamide 9 11 [33].

In the present study, poly (ethylene-co-methyl acrylate) (EMA) has been dispersed in a PP matrix. A second blend, containing the compatibilizing agent PP-g-MAH, has been synthesized. The nonisothermal crystallization

experimental data of the neat and blended systems, generated by differential scanning calorimetry (DSC), were fitted to three mackrokinetic models: Avrami, Tobin and Liu. The thermal properties of these blends are further investigated using thermogravimetric analysis (TGA) under an inert atmosphere. The characterization of PP/EMA blends also includes the determination of their tensile and impact properties, as well as their melt viscosities.

EXPERIMENTAL

Materials

PP used in this study (number-average molecular weight of 68,000 and weight-average molecular weight of 380,000) was purchased from Equate co., Kuwait. Maleic anhydride (reagent grade) and EMA (with MA content of 9 wt% and melt flow index of 2.6 g/10 min) were obtained from Sigma-Aldrich Pty. Ltd.

Blends Synthesis

PP and EMA were weighed and dried under vacuum at 80°C for 6 h. PP and EMA pellets (in the weight ratio 75/25%) were placed in plastic zipper bags, mixed by vigorous shaking and mechanically blended in a single-screw extruder at a screw speed of 75 rpm and barrel temperatures of 170, 185, 200 and 195°C from hopper to die. The strands from the extruder were immediately cooled in a water bath and pelletized. The pellets were dried for 6 h at 80°C in an oven.

Grafting of MAH onto PP was carried out in xylene with benzoyl peroxide. PP, MAH and xylene were heated with stirring in a vessel then benzoyl peroxide was added at once. The reaction continued for 4 hrs at 120°C under a steady flow of nitrogen. The reaction mixture was cooled, washed with methanol and dried in vacuum. Evidence for grafting was obtained from FTIR measurement. The graft ratio, determined from the weight increase, was approximately 2.7% based on the base polymer weight. The blend PP/PP-g-MAH/EMA [(PP75/EMA25)/PP-g-MAH 95/5 wt/wt%] was synthesized using single-screw extruder under the same conditions mentioned above.

Characterization

Nonisothermal Crystallization Studies

A Perkin-Elmer Diamond differential scanning calorimeter (DSC) was used to study the nonisothermal crystallization of PP, PP/EMA and PP/PP-g-MAH/EMA. Pure indium standard, having an equilibrium melting temperature (T_m^o)

of 156.6°C and an equilibrium enthalpy of fusion ((ΔH_f^o) of 28.5 $J \cdot g^{-1}$, was used for calibration. In a typical DSC experiment, a polymer sample was heated in the DSC furnace at 100°C/min from 30 to 200°C and held at that temperature for 5 minutes to eliminate the sample's thermal history. The sample was then cooled at one of the five cooling rates chosen (2.5, 5, 10, 20 and 40°C/min). The crystallization exotherms developed upon cooling were recorded for further analysis.

Thermal Stability

The thermal stability of the polymers under study was investigated using a SDT 2960 simultaneous DSC-TGA instrument. 7 ± 0.5 mg of polymer sample was heated from 30 to 800°C at a rate of 20°C/min under a steady flow of nitrogen (30 ml/min) to prevent oxidative reactions.

Mechanical Properties

The polymer pellets were injection molded into tensile specimens using Aruburg Allrounder injection molding machine. The mechanical characterization of the polymers was performed using Tinius Olsen H100KT universal testing machine. The testing was carried out in accordance with ASTM D638 at a speed of 20 mm/min for the determination of tensile strength and elongation and at 1 mm/min for the determination of Young's modulus. A Ray-Ran Universal Pendulum Impact Tester was utilized to obtain the impact strength of the polymer samples at ambient temperature in accordance with ASTM D256. At least five samples were tested in each of these investigations and the average values were reported.

Rheology

Melt rheological measurements were performed on RH2000 Bohlin Capillary Rheometer at a fixed temperature of 230°C in the shear rate range of 10^1–10^4 s^{-1}.

RESULTS AND DISCUSSION

Nonisothermal Crystallization Kinetics

It is assumed that the differential area under the crystallization curve obtained from DSC corresponds to dynamic changes in the conversion of the polymer mass from the melt phase to the solid phase. The crystallization kinetics can be analyzed by evaluating its degree of conversion as a function of temperature. The relative crystallinity, $\theta(T)$, or degree of conversion, can

be calculated according to the equation:

$$\theta(T) = \frac{\int_{T_o}^{T} (dH_c/dT)dT}{\int_{T_0}^{T_\infty} (dH_c/dT)dT} \tag{1}$$

where T is an arbitrary temperature, T_o is the crystallization onset temperature, T_∞ is the crystallization end temperature and dH_c is the enthalpy of crystallization.

In order to analyze the crystallization data with the models chosen, the temperature scale is transferred into a time scale using the following equation [31–33]:

$$t = \frac{T - T_o}{\beta} \tag{2}$$

where β is the cooling rate (°C/min) and t is the crystallization time at temperature T. The resulting function, $\theta(t)$, exhibits sigmoidal shapes and shows a dependence on the cooling rate. Figure 1 indicates that as the cooling rate increases, the time needed to attain complete relative crystallization decreases. This behavior is associated with the thermal activation of crystallization process [34].

Avrami equation is given as follows:

$$\theta(t) = 1 - \exp(-k_a t^{n_a}) \tag{3}$$

where k_a and n_a correspond to Avrami crystallization rate constant and Avrami exponent, respectively [23]. The Avrami kinetic parameters were

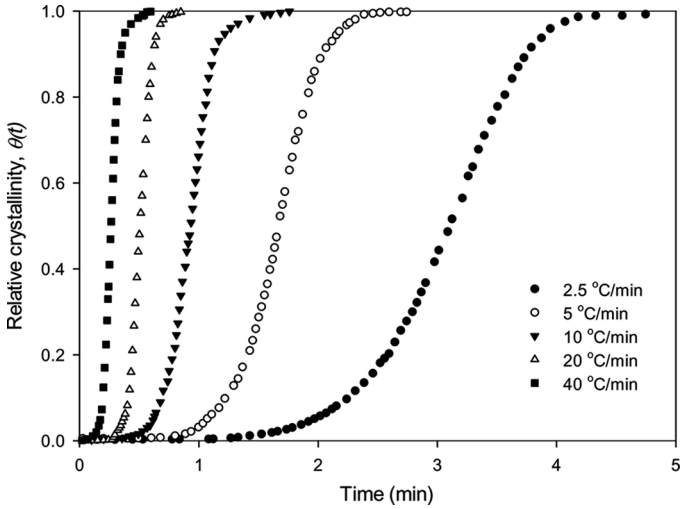

Figure 1: Relative crystallinity for the nonisothermal crystallization of PP/EMA at different cooling rates.

obtained by directly fitting equation (3) to the time-based experimental data. Figure 2 shows the application of Avrami model to the crystallization data of PP. It is obvious that the model predictions of relative crystallinity agree well with the overall experimental data, except for the final stages of crystallization. k_a and n_a values characterizing the crystallization of PP, PP/EMA and PP/PP-g-MAH/EMA are presented in Table 1. The high n_a values reflect the complex nature of crystal growth in the systems studied. The Avrami rate constant exhibits a clear proportional trend with cooling rate. The addition of EMA increases k_a values, indicating the enhancement of the crystallization rate of the blend. Compatibilization with PP-g-MAH also further improves the crystallization rate. This observation is also evident in Figure 3.

Tobin proposed a different expression describing the kinetics of phase transformation with an emphasis on growth impringement. The original theory was written in the form of a nonlinear Volterra integral equation, of which zeroth-order solution is given by Tobin [25]:

$$\theta(t) = \frac{(k_t t)^{n_t}}{1 + (k_t t)^{n_t}} \tag{4}$$

where k_t is the Tobin rate constant and n_t is the Tobin exponent. Tobin exponent n_t is governed by different types of nucleation and growth mechanisms. Figure 4 shows the application of Tobin model to the crystallization of PP/PP-g-MAH/EMA. The fitting seems less adhering to the data than that of Avrami. Tobin's kinetic parameters, resulting from the direct fitting of the experimental data to equation (4), are shown in Table 1. The n_t values are

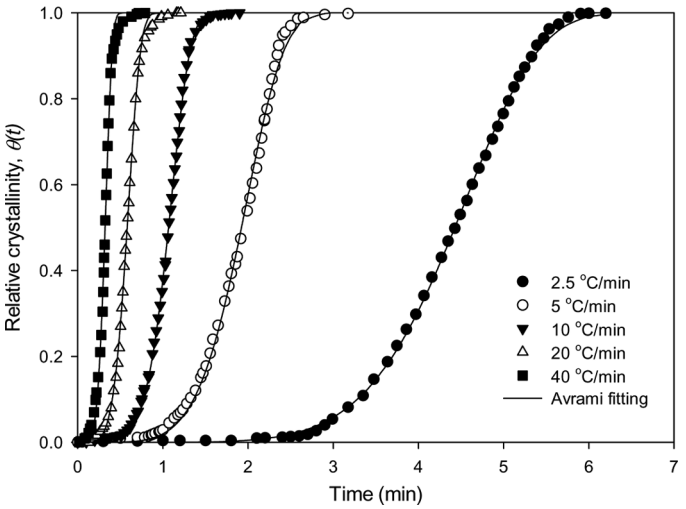

Figure 2: Application of Avrami model to the nonisothermal crystallization of PP at different cooling rates.

Table 1: Modeling nonisothermal crystallization data of PP, PP/EMA and PP/PP-g-MAH/EMA using Avrami and Tobin models.

System	Cooling rate (°C/min)	Avrami			Tobin		
		k_a (min^{-1})	n_a	*ASE*	k_t (min^{-1})	n_t	*ASE*
PP	2.5	5.4E−05	6.4	7.3E−05	0.17	9.5	9.1E−04
	5	0.02	5.4	3.5E−04	0.40	7.1	9.3E−04
	10	0.47	5.9	1.1E−04	0.95	8.5	8.7E−04
	20	8.0	5.2	1.8E−04	1.7	7.7	3.3E−04
	40	34.4	5.4	4.4E−04	3.1	8.0	7.4E−04
PP/EMA	2.5	6.8E−04	6.1	3.4E−05	0.21	8.8	6.6E−04
	5	0.03	6.3	1.1E−04	0.60	9.5	4.0E−04
	10	1.10	6.2	1.1E−04	1.1	9.0	3.3E−04
	20	13.0	6.9	3.0E−04	2.0	10.1	1.3E−04
	40	52.1	4.9	3.9E−04	5.0	2.9	2.7E−01
PP/PP-g-MAH/EMA	2.5	1.6E−03	5.7	4.8E−05	0.30	8.1	8.4E−04
	5	0.034	5.8	2.6E−04	0.60	7.5	1.6E−03
	10	2.1	6.4	3.4E−04	1.6	9.3	1.4E−03
	20	17.3	6.3	3.5E−04	3.6	8.8	3.1E−04
	40	71.5	5.6	9.3E−04	8.4	8.3	1.8E−04

considerably high, while the rate constant k_t varies only narrowly with the cooling rate. The increasing pattern between k_t and the cooling rate, though, is preserved. The blends, specially the compatibilized one, are characterized with higher rate constants. The accuracies of Avrami and Tobin models are represented in Figure 5. Avrami model follows the data quite well compared to Tobin model.

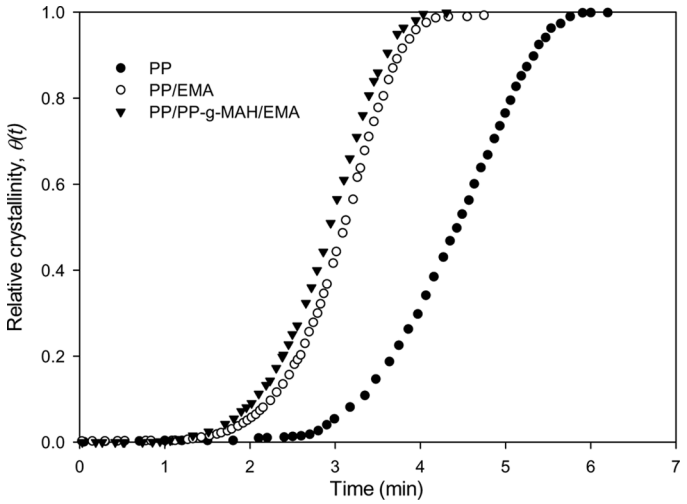

Figure 3: Relative crystallinity for the nonisothermal crystallization of PP, PP/EMA and PP/PP-g-MAH/EMA at a cooling rate of 2.5°C/min.

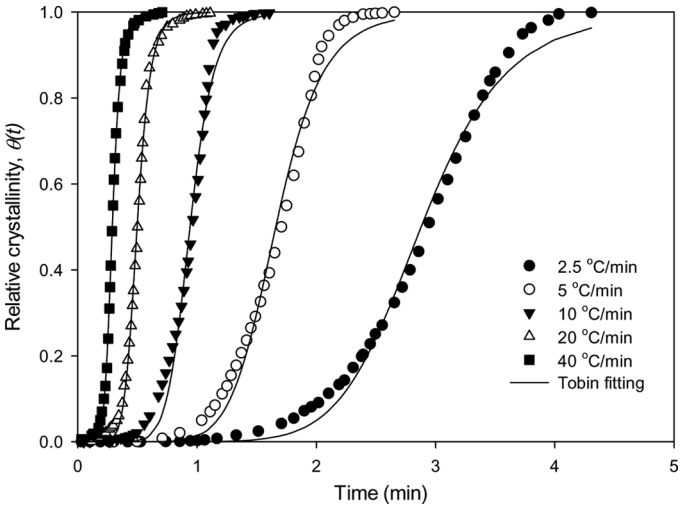

Figure 4: Application of Tobin model to the nonisothermal crystallization of PP/PP-g-MAH/EMA at different cooling rates.

The nonisothermal crystallization data of PP and its blends were also analyzed using Liu method, as per the equation given below [27]:

$$Ln(\beta) = Ln[F(T)] - aLn(t) \tag{5}$$

where $F(T)$ refers to the value of cooling rate that must be selected within a unit of crystallization time when the measured systems reach a certain degree

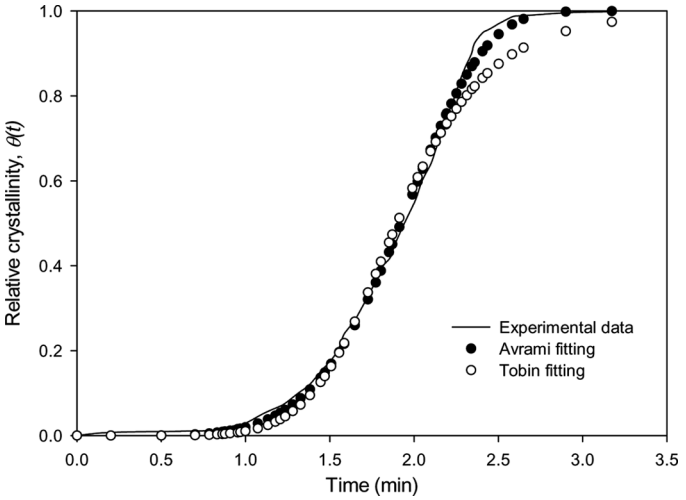

Figure 5: Avrami and Tobin fittings to the nonisothermal crystallization data of PP at 5°C/min.

Table 2: Modeling nonisothermal crystallization data of PP, PP/EMA and PP/PP-g-MAH/EMA using Liu method.

		Avrami		
System	**Relative crystallinity**	***a***	***F(T)***	***r***
PP	0.2	1.06	9.04	0.9939
	0.4	1.07	10.53	0.9945
	0.6	1.07	11.83	0.9957
	0.8	1.07	13.06	0.9954
PP/EMA	0.2	1.13	7.46	0.9986
	0.4	1.13	8.55	0.9996
	0.6	1.14	9.52	0.9997
	0.8	1.14	10.62	0.9999
PP/PP-g-MAH/EMA	0.2	1.21	7.24	0.9997
	0.4	1.19	8.63	0.9992
	0.6	1.18	9.68	0.9992
	0.8	1.19	10.81	0.9989

of crystallinity. a is the ratio of Avrami and Ozawa exponents. According to Eq. (5), at a given degree of crystallinity, plotting $Ln(\beta)$ versus $Ln(t)$ should yield a linear relationship. The kinetic parameters $F(T)$ and a are then obtained from the intercept and slope, respectively. The modeling results are shown in Table 2 and a representative plot is indicated in Figure 6. The good linearity displayed in this figure suggests that this model represents the data well. The values of $F(T)$ systematically increase with the increase in relative crystallinity, indicating that at unit of crystallization time, a higher cooling

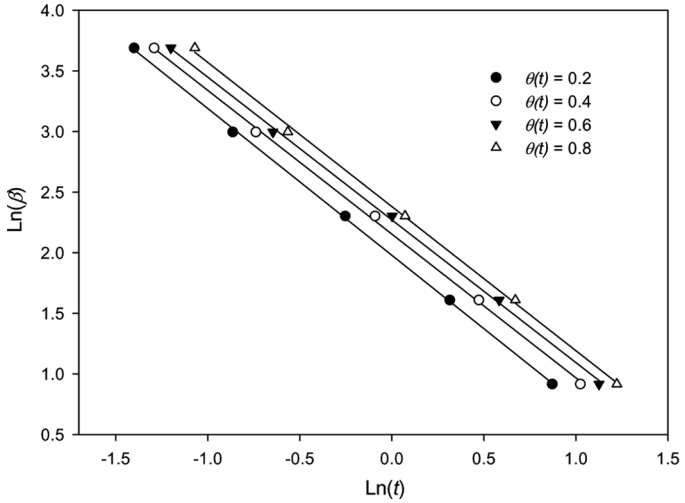

Figure 6: Application of Liu model to the nonisothermal crystallization of PP.

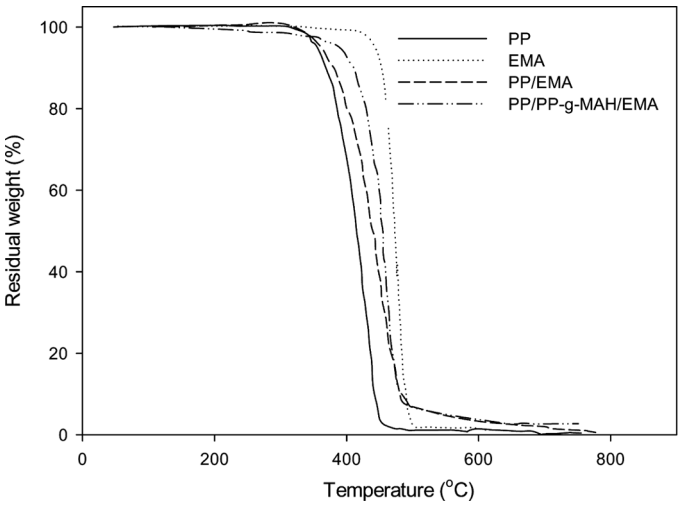

Figure 7: TG curves of PP, EMA, PP/EMA and PP/PP-g-MAH/EMA obtained at a heating rate of 20°C/min under nitrogen.

Table 3: Mechanical properties of PP, PP/EMA and PP/PP-g-MAH/EMA.

System	Yield strength (MPa)	Tensile strength (MPa)	Elastic modulus (MPa)	Ultimate elongation (%)	Impact strength (J/m)
PP	32	34	1000	99	46
PP/EMA	21	25	611	144	125
PP/PP-g-MAH/EMA	28	27	687	172	150

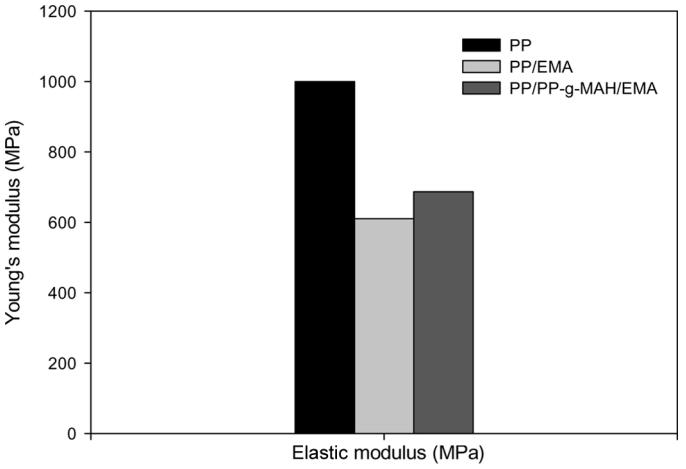

Figure 8: Young's modulus of PP, PP/EMA and PP/PP-g-MAH/EMA.

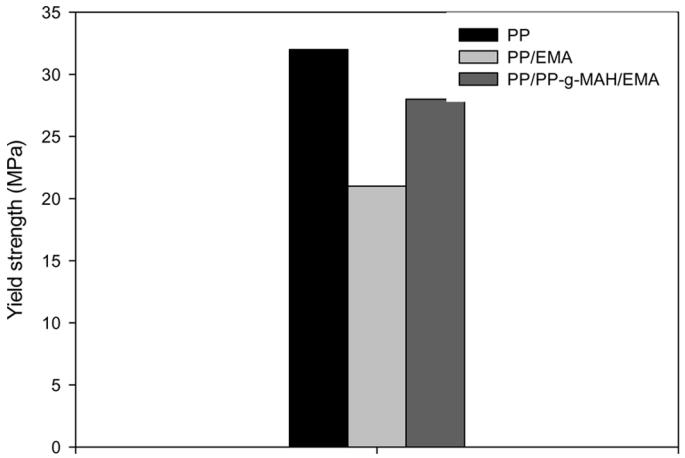

Figure 9: Yield strength of PP, PP/EMA and PP/PP-g-MAH/EMA.

rate should be used to obtain a higher degree of relative crystallinity. The values of α are almost constant for each system over the conversion range.

Thermal Stability

The thermograms of PP, EMA, PP/EMA and PP/PP-g-MAH/EMA are given in Figure 7. The incorporation of EMA into PP leads to increasing the thermal stability, as evident by the shift in initial degradation temperature to a higher temperature range. The compatibilized blend exhibits an enhancement in the thermal stability, compared to PP, but is still more susceptible to degradation than EMA.

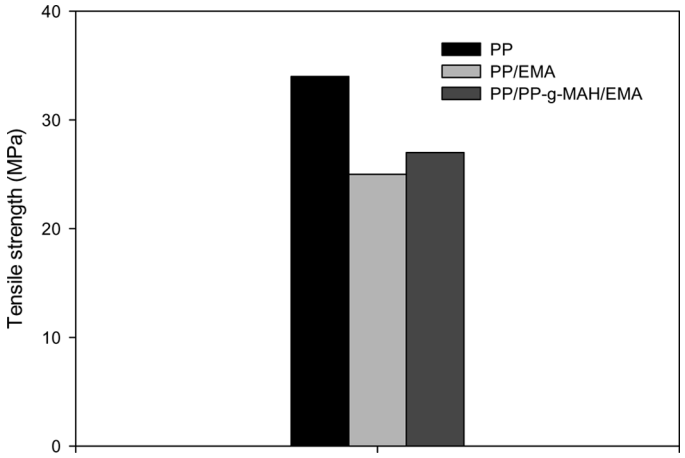

Figure 10: Tensile strength of PP, PP/EMA and PP/PP-g-MAH/EMA.

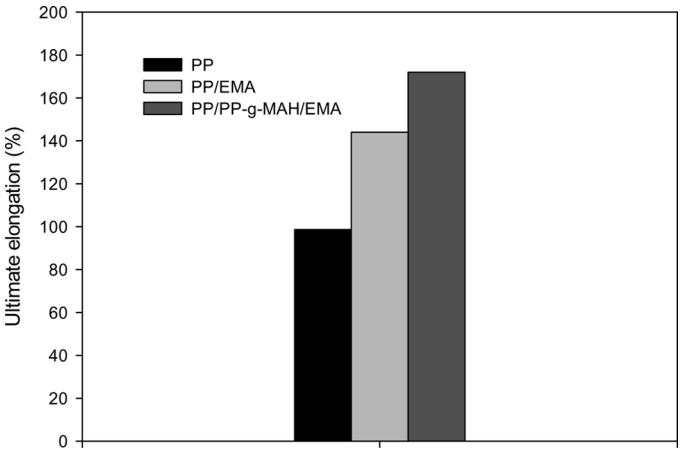

Figure 11: Ultimate elongation of PP, PP/EMA and PP/PP-g-MAH/EMA.

Mechanical Properties

The parameters determined from the mechanical testing of PP and its blends are summarized in Table 3. Young's modulus of PP deceases upon blending with EMA and only recovers marginally when a compatibilizer is added. This is indicated in Figure 8. PP-g-MAH gives a more noticeable contribution to the blend's yield strength, as shown in Figure 9. PP exhibits the highest tensile strength, followed by PP/PP-g-MAH/EMA and then PP/EMA. EMA. This is indicated in Figure 10. Ultimate elongation of PP, on the other side, shows a big increase when PP is blended with EMA (about 45%) and even a bigger increase when the blend is compatibilized (about 74%), as given in

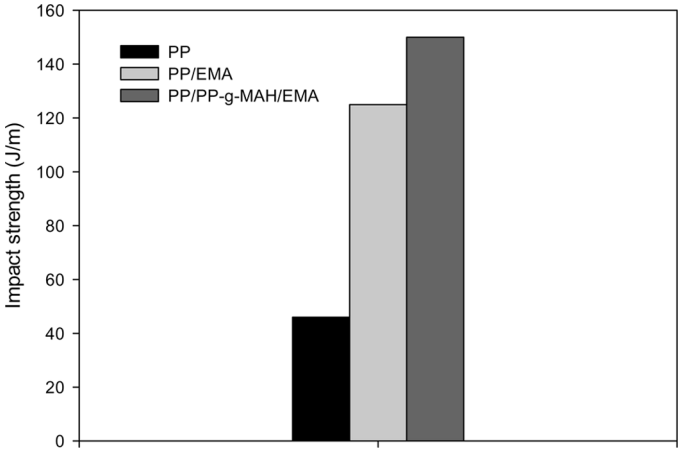

Figure 12: Impact strength of PP, PP/EMA and PP/PP-g-MAH/EMA.

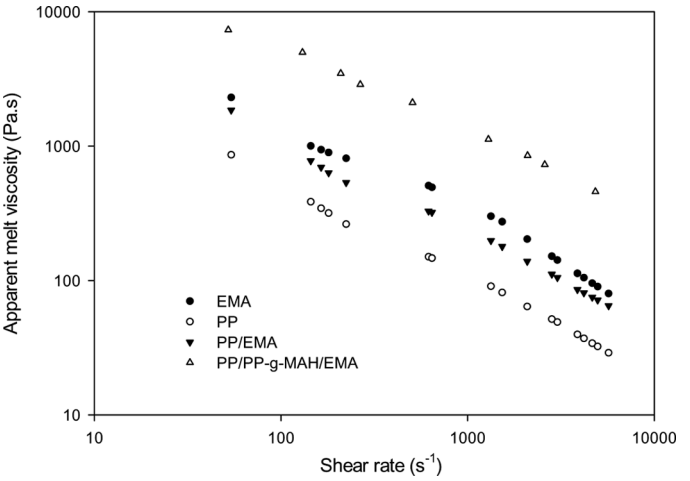

Figure 13: Apparent viscosity as a function of shear rate for PP, EMA, PP/EMA and PP/PP-g-MAH/EMA.

Figure 11. Another property that is enhanced with the incorporation of rubber is impact strength. Figure 12 reveals that the impact strength of PP/PP-g-MAH/EMA is 200% greater than that of PP. In summation, the addition of a compatibilizer to the PP/EMA blend leads to an increase in the blend's toughness, accompanied by a decrease in its stiffness. The trends in the mechanical properties are similar to those exhibited by PP/EPDM [16] and PP/EVA [19] blends.

Rheology

Melt viscosity as a function of shear rate for PP, EMA, PP/EMA and PP/PP-g-MAH/EMA is shown in Figure 13. The plots are quite linear for all the samples. All the molten polymers are non-Newtonian fluids and exhibit shear-thinning behavior. The viscosity function displayed by PP and its blends are typical of broad molecular weight distribution. Addition of EMA rubber resulted in an increase in the melt viscosity of PP.

CONCLUSION

In this study, blends of PP/EMA (75/25 wt/wt %) and (PP75/EMA25)/PP-g-MAH (95/5 wt/wt %) have been developed and characterized. The nonisothermal crystallization data obtained from differential scanning calorimetry were fitted to three models, Avrami, Tobin and Liu. Avrami and Liu were found to give more adequate fittings compared to Tobin. All models reflected the

crystallization rate enhancement induced by the addition of EMA to PP, which is attributed to the rubber's nucleation effect. Moreover, the compatibilization with PP-g-MAH further accelerated the crystallization of the blend. The high Avrami and Tobin exponent values indicate the complex nature of crystallization in the systems studied. All rate constants took on an increasing trend with increasing cooling rate. Avrami rate constant exhibited the strongest dependency on cooling rate. The thermal stability of PP, as determined by thermogravimetric analysis, showed an increase upon incorporation of EMA. The mechanical testing of PP and its blends revealed that the tensile strength (yield and ultimate) and Young's modulus decreased when PP was blended with EMA and did not change significantly with the addition of the compatibilizer. Impact strength and elongation, on the other hand, showed a tremendous increase for the blends compared to the neat components. The melt viscosities of the polymers displayed a non-Newtonian behavior over the range of shear rate studied. The compatibilization of these blends was found to increase the viscosity of the system, indicating an increase in interfacial adhesion.

REFERENCES

[1] Rohlmann, C. O., Failla, M. D., and Quinzani, L. M. *Polymer* **47**, 7795 (2006).

[2] Lotz, B., Graff, S., Straupe, C., and Wittmann, J. C. *Polymer* **32**, 2902 (1991).

[3] Hoffman, J. D. *Polymer* **24**, 3 (1985).

[4] Arranz-Andres, J., Pena, B., Benavente, R., Perez, E., and Cerrada, M. L. *Eur. Poly. J.* **43**, 2357 (2007).

[5] Joshi, J., Lehman, R., and Nosker, T. *J. Appl. Polym. Sci.* **99**, 2044 (2005).

[6] Ling, Z., Zhenghua, W., Rui, H., Liangbin, L., and Xinyuan, Z. *J. Mater. Sci.* **37**, 2615 (2002).

[7] Tjong, S. C., Xu, A. I., Li, R. K. Y., and Mai, Y. W. *J. Appl. Polym. Sci.* **87**, 441 (2002).

[8] Bai, H., Wang, Y., Zhang, D., Xiao, C., Song, B., Li, Y., and Han, L. *Mater. Sci. Eng.: Part A* **22**, 513–514 2009.

[9] Choudary, V., Varma, H. S., and Varma, I. K. *Polymer* **32**, 2534 (1991).

[10] Katbab, A. A., Nazockdast, H., and Bazgir, S. *J. Appl. Polym. Sci.* **75**, 1127 (2000).

[11] Walker, B. M. (1979). *Handbook of Thermoplastic Elastomers*, Van Nostrand Reinhold, New York, pp. 115–205.

[12] Verhoogt, H., Langelaan, H. C., Van Dam, J., and De Boer, A. P. *Polym. Eng. Sci.* **33**, 754 (2004).

[13] Da Costa, S. C. G., Goncalves, M. D. C., and Felisberti, M. I. *J. Appl. Polym. Sci.* **72**, 1827 (1999).

[14] Starke, J. K., Soares, B. G., Gorelova, M. M., Danesi, S., and Porter, R. S. *Polymer* **19**, 448 (1978).

[15] Do, I. H., Yoon, L. K., Kim, B. K., and Jeong, H. M. *Eur. Polym. J.* **32**, 1387 (1996).

[16] D'Orazio, L., Mancarella, C., Martuscelli, E., and Polato, F. *Polymer* **32**, 1186 (1991).

[17] Sengers, W. G. F., Sengupta, P., Noordermeer, J. W. M., Picken, S. J., and Gotsis, A. D. *Polymer* **45**, 8881 (2004).

[18] Denac, M., Musil, V., and Smit, I. *Compos. Part A: Appl. Sci. Manufac.* **36**, 1282 (2005).

[19] Thomas, S. *Mater. Letter* **5**, 360 (1987).

[20] Valera-Zaragoza, M., Ramirez-Vargas, E., Medellin-Rodriguez, F. J., and Huerta-Martinez, B. M. *Polym. Degrad. Stab.* **91**, 1319 (2006).

[21] De Loor, A., Cassagnau, P., Michel, A., and Vergnes, B. *J. Appl. Polym. Sci.* **53**, 1675 (1995).

[22] Pesneau, I., Michel, C., and Michel, H. *Polym. Eng. Sci.* **42**, 2016 (2002).

[23] Avrami, M. *J. Chem. Phys.* **7**, 1103 (1939).

[24] Malkin, A. Y., Beghishev, V. P., Keapin, I. A., and Bolgov, S. A. *Polym. Eng. Sci.* **24**, 1396 (1984).

[25] Tobin, M. C. *J. Polym. Sci. Polym. Phys.* **15**, 2269 (1977).

[26] Ozawa, T. *Polymer* **12**, 150 (1971).

[27] Liu, T., Mo., Z. S., Wang, S., and Zhang, H., *Polym. Eng. Sci.* **37**, 568 (1997).

[28] Huang, J. W., Chang, C. C., Kang, C. C., and Yeh, M. Y. *Thermochim. Acta* **66**, 468 (2008).

[29] Dangseeyun, N., Srimoaon, P., Supaphol, P., and Nithitanakul, M. *Thermochim. Acta* **63**, 409 (2004).

[30] Supaphol, P. *Thermochim. Acta* **37**, 370 (2001).

[31] Rychly, J., and Janigova, I. *Thermochim. Acta* **215**, 211 (1993).

[32] Apiwanthanakorn, N., Supaphol, P., and Nithitanakul, M. *Polym. Test.* **23**, 817 (2004).

[33] Cui, X., Qing, S., and Yan, D. *Eur. Polym. J.* **41**, 3060 (2005).

[34] Manchado, M. A. L., Biogiotti, J., Torre, L., and Kenny, J. M. *J. Therm. Anal. Cal.* **61**, 437 (2000).